Electronic structure of Yb compounds probed by hard X-ray photoemission spectroscopy

Yb compounds exhibit interesting physical properties originating from the hybridization between localized 4*f* electrons and itinerant conduction electrons (c–f hybridization). When the c–f hybridization is weak, the Ruderman-Kittel-Kasuya-Yosida interaction, where the 4*f* moments at different Yb sites interact indirectly mediated by the conduction electrons, is dominant and a magnetic order is realized at low temperatures. In contrast, when the c–f hybridization is strong, the Kondo effect becomes dominant and the 4*f* moments are screened with the conduction electrons, leading to a nonmagnetic ground state. The situation is summarized in the Doniach phase diagram [1]. The boundary point separating the magnetic and nonmagnetic ground state regions defines the quantum critical point (QCP). Unconventional physical phenomena such as superconductivity and a non-Fermi liquid state, where the electrical resistivity and specific heat, for example, show temperature dependences different from those in the normal metals, are observed near the QCP. In the study of 4*f* electron systems, one of the most important issues is to establish the electronic structure around the QCP.

$YbNi_3X_9$ and $Yb_2Pt_6X_{15}$ (X = Al, Ga) are suitable systems for investigating the change in electronic structure across the QCP. $YbNi_3Al_9$ exhibits magnetic order below 3.4 K, while $YbNi_3Ga_9$ shows no magnetic order. $YbNi_3Al_9$ and $YbNi_3Ga_9$ thus occupy the weak and strong c–f hybridization regions, respectively, across the QCP in the Doniach phase diagram, in spite of having the same crystal structure and similar conduction electronic states. Although $YbNi_3X_9$ and $Yb_2Pt_6X_{15}$ have similar crystal structures and are both located in the nonmagnetic region, magnetic susceptibility measurements indicate that $Yb_2Pt_6Al_{15}$ is closer to the QCP than $Yb_2Pt_6Ga_{15}$. Thus, $YbNi_3X_9$ and $Yb_2Pt_6X_{15}$ provide an opportunity to systematically investigate the change in electronic structure in moving from magnetic (weak c–f hybridization) to nonmagnetic (strong c–f hybridization) regions in the Doniach phase diagram across the QCP. In this study, we carried out hard X-ray photoemission spectroscopy (HAXPES) measurements at hν = 5.95 keV on $YbNi_3X_9$ and $Yb_2Pt_6X_{15}$ at SPring-8 **BL15XU** [2,3].

The Yb $3d_{5/2}$, Ni $2p_{3/2}$ ($YbNi_3X_9$) and Pt $4f_{7/2}$ ($Yb_2Pt_6X_{15}$) and valence-band HAXPES spectra of $YbNi_3X_9$ and $Yb_2Pt_6X_{15}$ measured at 20 K showed similar X-dependences (Fig. 1) as follows. The Yb $3d_{5/2}$ spectrum is split into the Yb^{2+} ($4f^{14}$) and Yb^{3+} ($4f^{13}$) parts. The Yb^{2+} peak is very tiny for X = Al and is enhanced for X = Ga, indicating that the Yb valence is shifted from almost trivalent toward divalent states. The Ni $2p_{3/2}$ and Pt $4f_{7/2}$ peaks for X = Ga are located at a lower binding energy (E_B) than those for X = Al. The same energy shift is observed for the Ni 3*d* and Pt 5*d* structures in the valence-band spectra. In contrast, the opposite energy shift is observed in the Yb^{3+} 4*f* multiplet.

The similar X-dependent spectra of $YbNi_3X_9$ and $Yb_2Pt_6X_{15}$ suggest some systematic changes in electronic structure in moving from weak (X = Al) to strong (X = Ga) c–f hybridization regions in the Doniach phase diagram. A simple electronic model (Fig. 2) qualitatively explains these experimental results. The

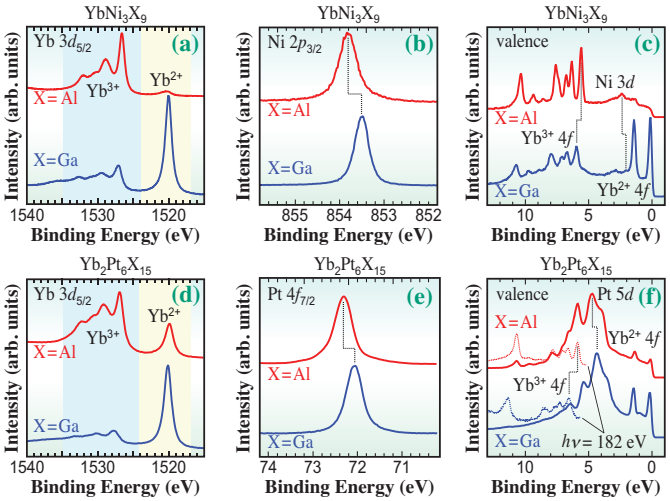

Fig. 1. **(a)** Yb $3d_{5/2}$, **(b)** Ni $2p_{3/2}$ and **(c)** valence-band HAXPES spectra of $YbNi_3X_9$ and **(d)** Yb $3d_{5/2}$, **(e)** Pt $4f_{7/2}$ and **(f)** valence-band HAXPES spectra of $Yb_2Pt_6X_{15}$ measured at 20 K. The spectra at $h\nu = 182$ eV obtained at BL-7 of HiSOR to enhance the Yb^{3+} 4*f* peak are also presented in (f).

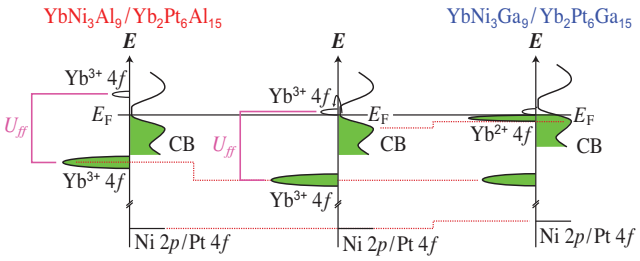

Fig. 2. Electronic model of $YbNi_3X_9$ and $Yb_2Pt_6X_{15}$ for X = Al (left) and X = Ga (right). The middle figure connects the left and right figures.

Yb 4*f* and conduction-band densities of states (DOS) are drawn at the left and right sides of the energy axis, respectively. The Yb^{3+} 4*f* level is split into the occupied and unoccupied levels at the energy distance of the Coulomb interaction energy between the 4*f* electrons (U_{ff}). The 4*f* hole level for X = Al is located far above the Fermi energy (E_F), and the Yb valence is close to 3. On going from X = Al to X = Ga, the 4*f* hole level becomes closer to E_F, and as a result, the occupied 4*f* level is shifted to higher E_B side, as observed in the experiments. The conduction electrons are easily transferred to the 4*f* hole just above E_F, and some Yb^{3+} ions change to Yb^{2+} ions and the Yb^{2+} $4f_{7/2}$ peak appears just below E_F. With the transfer of conduction electrons, E_F shifts to a smaller value in the conduction-band DOS. This E_F shift leads to the Ni $2p_{3/2}$ and Pt $4f_{7/2}$ shifts to lower E_B. Thus, the X-dependent HAXPES spectra of $YbNi_3X_9$ and $Yb_2Pt_6X_{15}$ are both understood in terms of the simple electronic model (Fig. 2).

Recently, a resonant HAXPES (rHAXPES) technique has been developed at SPring-8 **BL09XU** as a Partner User Proposal (PI: Prof. K. Mimura, Osaka Prefectural University). The Yb $3d_{5/2}$ HAXPES spectra (Figs. 1(a) and 1(d)) were obtained at a fixed photon energy. When an incident photon energy is tuned at the Yb L_3 edge (8.94 keV), a resonant behavior in the Yb^{2+} and Yb^{3+} peaks is expected. The detailed analysis of the resonant behavior provides the Coulomb interaction energy between the localized 4*f* and itinerant 5*d* electrons (U_{fd}), which is related to the Yb valence. Here, we present rHAXPES results for $YbInCu_4$ [4] with a valence transition at T_V = 42 K, where the Yb valence abruptly changes from 2.90 to 2.74 on cooling. The present results obtained at BL09XU are first reported for Yb L_3 rHAXPES. Figure 3(a) shows the Yb $3d_{5/2}$ rHAXPES spectra measured at 20 K with hν varied from 8915 to 8965 eV. Clear resonant enhancement is successfully detected both for the Yb^{2+} and Yb^{3+} peaks around the Yb L_3 edge. Figure 3(b) shows the Yb^{2+} and Yb^{3+} peak intensities as a function of hν, called constant initial state (CIS) spectra. The Yb^{2+} and Yb^{3+} CIS spectra exhibit similar behaviors. As hν increases from 8915 eV, the intensity gradually decreases. After reaching a minimum, the intensity rapidly attains a maximum and then again decreases. The CIS spectra are well fitted with the Fano profile given by $(E+q)^2/(E^2+1)$ with $E = (h\nu - E_0)/\Gamma$, where E_0, Γ and *q* are the resonant photon energy, the half-width of the resonance and the asymmetry parameter, respectively.

The Yb^{2+} CIS spectrum is shifted to a lower photon energy than the Yb^{3+} CIS spectrum. The amount of energy shift provides information on U_{fd}, which plays an important role in the valence transition. In the present experiment, no clear change between the CIS spectra measured at 20 and 70 K across the valence transition was detected. To enable further discussion, a theoretical calculation based on the single impurity Anderson model is in progress.

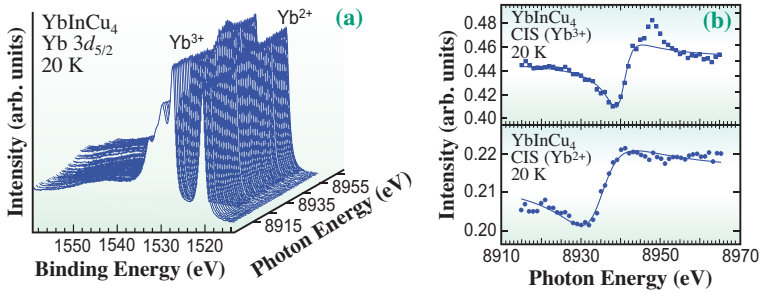

Fig. 3. **(a)** *hν* dependence of Yb $3d_{5/2}$ rHAXPES spectra around the Yb L_3 edge of $YbInCu_4$ measured at 20 K. **(b)** CIS spectra of Yb^{3+} (squares, upper panel) and Yb^{2+} (circles, lower panel) components in the Yb $3d_{5/2}$ rHAXPES spectra in (a). The Fano profiles are shown by line curves.

Hitoshi Sato

Hiroshima Synchrotron Radiation Center,
Hiroshima University

Email: jinjin@hioshima-u.ac.jp

References

[1] S. Doniach: Physica B+C **91** (1977) 231.
[2] Y. Utsumi *et al.*: Phys. Rev. B **86** (2012) 115114.
[3] A. Rousuli *et al.*: Phys. Rev. B **96** (2017) 045117.
[4] *K. Maeda, H. Sato, Y. Akedo, T. Kawabata, K. Abe, R. Shimokasa, A. Yasui, M. Mizumaki, N. Kawamura, E. Ikenaga, S. Tsutsui, K. Matsumoto, K. Hiraoka and K. Mimura: JPS Conf. Proc.* ***30*** *(2020) 011137.*